Chapter 4

Design of Fluorescent Fusion Protein Probes

Elizabeth Pham and Kevin Truong

Abstract

Many fluorescent probes depend on the fluorescence resonance energy transfer (FRET) between fluorescent protein pairs. The efficiency of energy transfer becomes altered by conformational changes of a fused sensory protein in response to a cellular event. A structure-based approach can be taken to design probes better with improved dynamic ranges by computationally modeling conformational changes and predicting FRET efficiency changes of candidate biosensor constructs. FRET biosensors consist of at least three domains fused together: the donor protein, the sensory domain, and the acceptor protein. To more efficiently subclone fusion proteins containing multiple domains, a cassette-based system can be used. Generating a cassette library of commonly used domains facilitates the rapid subcloning of future fusion biosensor proteins. FRET biosensors can then be used with fluorescence microscopy for real-time monitoring of cellular events within live cells by tracking changes in FRET efficiency. Stimulants can be used to trigger a range of cellular events including Ca^{2+} signaling, apoptosis, and subcellular translocations.

Key words: FRET biosensors, fusion proteins, computational modeling, cell imaging, structure-based design.

1. Introduction

Biosensors relying on the fluorescence resonance energy transfer (FRET) between fluorescent proteins have been used extensively, including for live-cell imaging of cellular events such as caspase activation, protein phosphorylation, and calcium ion (Ca^{2+}) signaling (1–7). FRET is the natural phenomenon of energy transfer via resonance between two fluorophores with a spectral overlap between the donor emission and the acceptor excitation. The efficiency of this energy transfer depends on the relative distance and orientation between the donor and acceptor (8). In FRET

D.B. Papkovsky (ed.), *Live Cell Imaging*, Methods in Molecular Biology 591,
DOI 10.1007/978-1-60761-404-3_4,

protein biosensors, natural sensory proteins for the desired cellular events are inter- or intramolecularly fused with a pair of fluorescent proteins of suitable spectral overlap, such as cyan fluorescent protein (CFP) as the donor and yellow fluorescent protein (YFP) as the acceptor (2, 9). The efficiency of energy transfer between the donor and acceptor fluorescent proteins becomes altered by conformational changes of a fused sensory protein caused by a cellular event. Hence, a change in FRET efficiency of a biosensor can be correlated with the cellular event.

In the case of FRET Ca^{2+} biosensors, changes in FRET efficiency can be correlated with Ca^{2+} concentrations (10–13). CFP and YFP have been genetically fused with calmodulin (CaM), a cytoplasmic Ca^{2+}-sensitive protein. Upon binding Ca^{2+} ions, CaM undergoes a conformational change from an extended to a compact conformation by wrapping around a fused CaM-binding peptide (14, 15), which alters the relative distance and orientation of the FRET pair. As a result, an increase in FRET efficiency corresponds to a higher ion concentration. Different configurations of fusion proteins can be used to monitor different cellular events. A fusion construct of a peptide fused between two fluorescent proteins can be used to observe proteolytic cleavage, where a decrease in FRET efficiency would correspond to a cleavage event (16). In the presence of protease proteins, the biosensor is cleaved, separating its fluorescent pair and causing a loss in FRET efficiency.

1.1. Structure-Based Computational Modeling

The design of fluorescent probes is often dependent on the structure of the sensory domain chosen. With available structural information, a computational model can be constructed to assist in the design process. This structure-based design of fluorescent probes allows existing probes to be better designed to have improved dynamic ranges. The NMR structure of CaM bound to a CaM-binding peptide from CaM-dependent kinase kinase was used to improve existing CaM-based biosensors. A computational model of CaM bound to its peptide showed that it would be possible to splice the peptide within the CaM structure to improve the dynamic range attainable (17). Similarly, the structure of caspase-3 bound to its inhibitor peptide was used to computationally design an improved caspase-3 activation biosensor (18, 19).

A computational modeling tool can thus be developed to estimate FRET efficiency changes. We previously developed a computational tool called FPMOD (Fusion Protein MODeler) to predict FRET efficiency changes of a range of biosensor constructs. FPMOD can be used to generate fusion protein models from PDB (protein databank) files containing the three-dimensional structures of proteins and other biological macromolecules. By defining regions of flexible linkers between different domains and then rotating the domains around these flexible linkers to

produce random conformations, FPMOD samples the conformational space of a biosensor design and provides average predicted FRET efficiency changes. These predicted values can then be used to evaluate potential biosensor designs (13, 20).

1.2. Cassette System

To create fusion proteins, subcloning techniques are employed to insert PCR products of individual domains into an expression vector at restriction enzyme cut sites. The availability of these sites limits the number and configuration of the biosensor constructs possible. Future fusions of other domains into existing vectors are not always possible due to available restriction sites either exhausted in previous subcloning steps or incompatible. To more efficiently construct fusion proteins containing multiple domains, a cassette-based system can be used. Cassettes will have a standard vector structure based on specific restriction endonuclease sites that can be used to fuse domains in any configuration and number of times. If properly designed, this cassette vector can also be used to simplify the process of screening successful recombination of insertion fragments using fluorescence (21).

Specifically for FRET biosensors, often at least three domains will need to be fused together: the donor protein, the sensory domain, and the acceptor protein. Generating a cassette library of commonly used domains (e.g., CFP and YFP) facilitates the rapid subcloning of fusion biosensor proteins that can be recombined any number of times irrespective of order while maintaining the same simple management of restriction sites.

1.3. Live-Cell Imaging Using Fluorescence Microscopy

Fluorescence microscopy allows the real-time monitoring of cellular events within live cells by tracking the change in FRET efficiency. Stimulants can be used to trigger cellular events such as Ca^{2+} signaling, apoptosis, and subcellular translocations (16, 22–24). Simultaneous signaling processes can also be observed using a co-culture of cells transfected with different FRET biosensors (22). An advantage of live-cell imaging with fluorescence is the real-time monitoring of molecular signaling pathways using FRET biosensors and any corresponding morphological changes (16).

2. Materials

2.1. Structure-Based Computational Modeling

1. Software used to develop FPMOD (individual.utoronto.ca/ktruong/software.htm): C++ Development Environment – Bloodshed Dev-C++ IDE (www.bloodshed.net/devcpp.html), Perl language platform – ActivePerl (www.activestate.com/Products/activeperl/index.mhtml),

gGraphical uUser iInterface (GUI) – wxWindows toolkit (sourceforge.net/projects/wxwindows).

2. Structural resources: Protein 3D structure – protein databank (PDB) files (www.rcsb.org), 3D structure viewing – Swiss PDB viewer (www.expasy.ch/spdbv/text/getpc.htm), protein structure manipulation and rendering – PyMOL (pymol.sourceforge.net).

2.2. Cassette System

1. Base vectors: pTriEx 1.1 – Hygro (Novagen, Madison, WI, USA), designed primers (Invitrogen, Carlsbad, CA, USA).
2. Subcloning enzymes (*see* **Note 1**): restriction enzymes *Nco*I, *Spe*I, *Bam*HI, *Stu*I, *Bgl*II, *Sma*I, *Nhe*I, *Pme*I, *Xho*I (New England Biolabs, Ipswich, MA, USA), ligation enzyme T4 DNA ligase (New England Biolabs), and *Pfu* DNA polymerase (Fermentas, Burlington, ON, Canada) with 5 mM deoxyribonucleotide (dNTP) mixture (Fermentas).
3. Subcloning equipment: PCR amplification Mastercycler Personal system (Eppendorf, Mississauga, ON, Canada), Mini Electrophoresis system for DNA electrophoresis (VWR, Mississauga, ON, Canada).
4. DNA purification kits: PureLink Quick Plasmid Miniprep kit, PureLink PCR Purification kit, and PureLink Gel Extraction kit with 1% UltraPure agarose gel in Tris-acetate–EDTA buffer (0.5× TAE bBuffer) (Invitrogen). Ethidium bromide (Sigma-Aldrich, Oakville, ON, Canada), O'GeneRuler DNA Ladder Mix (Fermentas) and Electronic UV transilluminator (Ultra Lum, Inc., Claremont, CA).
5. Bacterial transformation and growth reagents: *Escherichia coli* DH5α strain competent cells (Subcloning Efficiency, Invitrogen) grown in Luria broth (LB) (Sigma-Aldrich) with 100 μg/mL ampicillin (Sigma-Aldrich) and plated on LB agar plates (Sigma-Aldrich) with 100 μg/mL ampicillin (Sigma-Aldrich) grown in a shaking incubator (Barnstead, Dubuque, IA).
6. Fluorescence screening of bacterial cells: Lighttools Illuminatool Tunable Lighting System LT-9500 (Lighttools Research, Encinitas, CA) equipped with 535 and 470 nm viewing filters and 488/10 and 440/10 nm filter cups.
7. Protein purification: Ni-NTA 6% agarose beads charged with Ni^{2+} ions (Qiagen, Valencia, CA).

2.3. Live-Cell Imaging Using Fluorescence Microscopy

1. Cell culture reagents (*see* **Note 2**): Cos-7 cells, Dulbecco's Modified Eagle Medium (DMEM) with high glucose, L-glutamine and sodium pyruvate (Invitrogen), fetal bovine serum (FBS) (Sigma-Aldrich), trypsin–EDTA (Sigma-Aldrich), cell freezing medium dimethyl sulfoxide

(DMSO) (Sigma-Aldrich), Dulbecco's phosphate-buffered saline (PBS) without Ca^{2+}, Mg^{2+}, or phenol red (Invitrogen), PBS with Ca^{2+} (Invitrogen), and Lipofectin Transfection Reagent (Invitrogen) (stored at 4°C).

2. Materials for cell culture: T-25 flasks (Sarstedt, Montreal, QC, Canada) and 35-mm glass-bottom dishes (MatTek, Ashland, MA).
3. Stimulants (*see* **Note 1**): Ionomycin (1 μM in PBS) (Sigma-Aldrich), ATP (10 μM in PBS) (Fermentas), and Staurosporine (STS) (5 μM in PBS) (Sigma-Aldrich).
4. Microscope: Inverted microscope IX81 with Lambda DG4 Xenon lamp source and CCD camera, objective (10×), oil-immersion objectives (20×, 40×, 60×, 100×) (Olympus, Markham, ON, Canada) (*see* **Note 3**), filter sets (BRIGHTLINE CFP FILTER SET EX:438/24, 458DM, EM:483/32, BRIGHTLINE YFP FILTER SET EX:500/24, 520DM, EM:542/27) (Semrock, Rochester, NY), 2-channel filter for simultaneous dual-band imaging of CFP and YFP (Roper Biosciences SpecEM, Tucson, AZ).
5. Imaging software packages: QEDInVivo and ImagePro-Plus (MediaCybernetics, Bethesda, MD).

3. Methods

3.1. Structure-Based Computational Modeling

The prediction of FRET efficiency changes of potential candidate biosensor constructs prior to subcloning helps to determine which constructs will likely have an appropriate dynamic range for the specific application. A computational modeling tool such as FPMOD (13) can be developed to construct fusion proteins based on determined atomic structural information from PDB files. The modeling tool should allow the sampling of a biosensor's conformational space and estimate the FRET efficiency change in response to a stimulus. This requires that structures are available for domains and proteins before and after the desired cellular event. Estimated values provided should include the distance factor, orientation factor, and FRET efficiency for each candidate biosensor. These values are sufficient to compare the candidate biosensor constructs and to select the construct that should be subcloned in vitro and tested further.

FRET efficiency (E%) is the percentage of energy transferred between a donor–acceptor fluorophore pair. This efficiency is a function of the Forster distance factor, R_o, the distance between the fluorophores, R, and the orientation factor, κ^2. In turn, the orientation factor depends on the angle between donor or

acceptor fluorophore dipoles and the joining vector (θ_A and θ_D, respectively), as well as the angle between fluorophore pair planes (α). A common assumed constant for κ^2 is $2/3$ but this does not apply here because the linkers within the biosensors are not in isotropic motion upon Ca^{2+} binding (25, 26). Several relevant parameters are constants defined for the donor–acceptor pair used in the biosensor. For CFP and YFP, these constants are quantum yield ($Q_D = 0.42$), refractive index ($n = 1.4$), and overlap integral ($J = 1.46\text{e-}9$). For each conformation, the dipoles and related angles were determined from the PDB files and used in Equations [1], [2], and [3] to determine R, κ^2, and E%.

$$E\% = \frac{R_0^6}{R_0^6 + R^6} \quad [1]$$

$$R_0 = 9.78 \times 10^3 \times \left(Q_d \kappa^2 n^{-4} J\right)^{1/6} \text{Å} \quad [2]$$

$$\kappa^2 = [\sin(\theta_D)\sin(\theta_A)\cos(\phi) - 2\cos(\theta_D)\cos(\theta_A)]^2 \quad [3]$$

The orientation of transition dipoles is defined with respect to PDB atom coordinates of the HETATM for CFP and YFP, from atom N15 to C4 and N3 to CZ, respectively. This assumed direction is kept consistent for all constructs simulated. For other donor–acceptor fluorescent pairs, the transition dipoles will need to be determined from their PDB files.

A graphical user interface (GUI) should be developed to simplify use of the modeling tool. It should include at least the following features: custom dialog boxes to ensure that the user will enter the necessary arguments and an output window for viewing results. Such a GUI can be developed using the wxWindows toolkit (wxWidgets Open Source Software).

3.1.1. High-Level Organization of FRET Biosensor Modeling Tool

1. The solved atomic structure of each domain of a FRET biosensor construct must be available. Most importantly, the structure of the sensory domain before and after the desired cellular event must be available as separate structural files.
2. Domains are treated as rigid bodies while linkers fusing the domains together are considered flexible.
3. To generate the conformational space of a biosensor construct, a sufficient number of models must be generated where rigid-body domains are rotated around the flexible linkers. For each residue in a linker, there are three torsional or dihedral angles: ψ, Φ, and ω. During a random rotation step, all linker residues are randomly rotated such that all atoms of a linker residue preceding the N atom along the N–C_α bond are rotated by the torsional angle Φ. Next, all atoms after the C atom along the C_α–C bond are rotated by

angle ψ. While the angles ψ and Φ do not have any restriction so that they range from –180° to 180°, ω is fixed at 180°. These dihedral angles are given random values, representing a random rotation of each peptide bond within the user-defined flexible linkers.

4. Valid conformations must be screened from the collection of randomly generated conformations. This involves selecting only conformations whose atoms do not sterically collide after random rotations of the linker regions. Each randomly generated model is then saved as individual PDB files.
5. This linker rotation procedure is repeated until a representative number of models are generated to sufficiently span the conformational space (*see* **Note 4**).
6. From each PDB file generated previously, the distance factor, orientation factor, and FRET efficiency estimations can be tabulated.

3.1.2. Structure-Based Computational Design Process

1. Determine availability of solved atomic structures for all domains and proteins used in fusion biosensor protein. For the sensory domain, structural information for both before and after a cellular event must be available.
2. Use modeling tool to construct the biosensor construct, defining domains as rigid bodies and linkers as flexible sequences with no secondary structure. Generate a sufficient collection of valid conformations. Determine the distance factor, orientation factor, and FRET efficiency value for each generated model. Tabulate values and average to determine a FRET efficiency value representing the conformational space of each candidate biosensor construct. Determine the conformational space and FRET efficiency value for the FRET biosensor before and after the desired cellular event.
3. Use the change in FRET efficiency to determine appropriateness of using the proposed biosensor construct for in vitro and cell imaging studies.

3.1.3. Example of the Use of the Computational Modeling Tool FPMOD to Design a New Class of Ca^{2+} Biosensor According to 3.1.2

1. Solved atomic structures for epithelial cadherin, CFP, and YFP were downloaded from the Protein Databank: 1MYW (Venus (27), a variant of YFP), 1OXD (CFP), 1EDH with Ca^{2+} removed and linkers defined as flexible (epithelial cadherin domain in the absence of Ca^{2+} ions), 1EDH (epithelial cadherin domain in the presence of Ca^{2+} ions).
2. Constructs were created in FPMOD (13) for CEcadY12 (**Fig. 4.1**) before and after Ca^{2+} binding. Average predicted values of the distance factor, orientation factor, and FRET efficiency were determined for 130 conformations each of

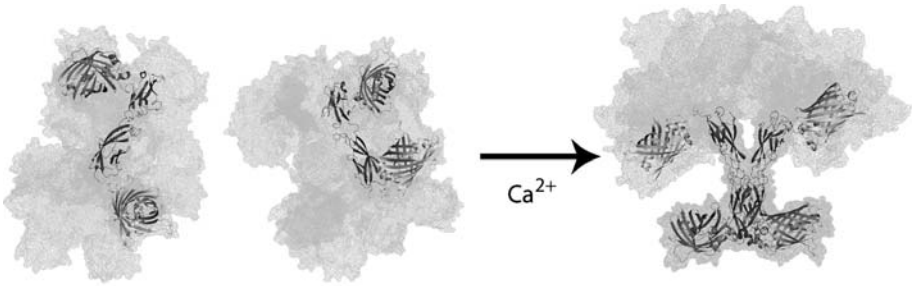

Fig. 4.1. Superposition of multiple conformations of the CEcadY12 biosensor in the presence and absence of Ca^{2+} binding. The conformational space conferred by generated models of possible conformations are shown for CEcadY12 before (*left*) and after (*right*) Ca^{2+} binding. After Ca^{2+} binding, biosensors homodimerize, forcing the CFP/YFP pair to move closer and increasing the FRET efficiency.

the unbound case (91 Å, 0.59, 3.1%) and bound case (85 Å, 0.39, 4.5%), respectively.

3. For CEcadY12, the FRET efficiency change predicted was an increase of 3.6% upon Ca^{2+} binding. FPMOD demonstrated that CEcadY12, which is a new class of Ca^{2+} biosensors, showed a sufficient predicted change in FRET efficiency to warrant further study. In vitro FRET efficiency measurements showed an increase of 14% upon binding of Ca^{2+}. The developed FRET biosensor can be used further in live-cell imaging studies (data not shown). Other relevant characteristics of a FRET biosensor can be discerned from the predicted values if desired (*see* **Note 5**).

3.2. Cassette System

3.2.1. Components of a Standard Cassette Vector

1. The standard cassette vector we created follows the scheme illustrated in **Fig. 4.2**. Restriction cut sites 2a and 2b should be sequences for different restriction enzymes that produce blunt or compatible cohesive ends such as *Spe*I/*Nhe*I, *Bam*HI/*Bgl*II, and *Stu*I/*Sma*I (more than one pair of compatible restriction enzymes can be included at this multiple cloning site). When these compatible cohesive ends are ligated together, the ligation product becomes unrecognizable by either restriction enzyme. Cut sites 1 and 3, however, should be sequences that produce unique cohesive ends on the vector such as *Nco*I and *Xho*I.
2. The standard cassette vector should also contain a gene for a fluorescent protein flanked by blunt-end restriction cut sites 4a and 4b such as *Pme*I.
3. The presence of the stop codon upstream of the fluorescent protein gene allows for quick, reliable screening of successful subclones and recombination by fluorescence. The vectors do not fluoresce when expressed because of the presence of the stop codon. However, when the stop codon is replaced

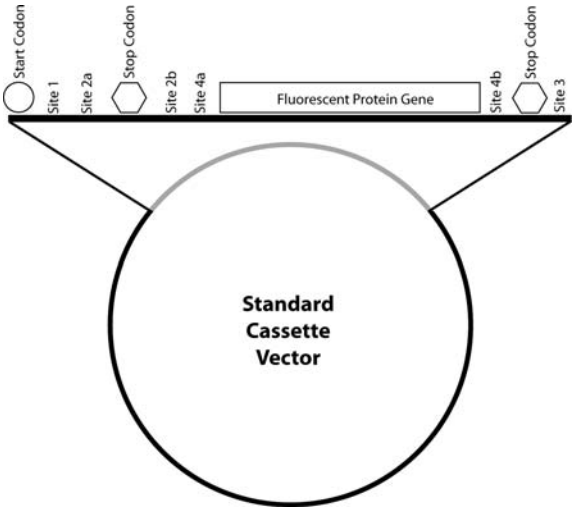

Fig. 4.2. Schematic diagram of a standard cassette vector. Restriction sites 1 and 3 should produce unique cohesive ends, such as *Nco*I and *Xho*I. Sites 2a and 2b should produce either blunt ends or compatible cohesive ends such as *Spe*I/*Nhe*I, *Bam*HI/*Bgl*II, and *Stu* I/*Sma* I. Multiple compatible restriction sites can be included in the vector at these sites. Finally, sites 4a and 4b should produce blunt ends to allow the removal of the fluorescent protein gene.

by a gene of interest, the fluorescent protein gene will be expressed, indicating a successful subclone.

4. If a non-fluorescent cassette is desired, the fluorescent protein gene can be easily removed by cutting at blunt-end sites 4a and 4b followed by a self-ligation.

3.2.2. Construction of a Standard Cassette Vector – pCfvtx

1. Our standard expression vector, pCfvtx (21), was created from pTriEx 1.1 – Hygro and pVenus (27) (*see* **Notes 6** and **7**).
2. Primers were used to PCR amplify the Venus gene with the restriction enzyme sequences for *Nco*I, *Spe*I, *Nhe*I, and *Pme*I upstream of Venus (5′-CATGCCATGGG-CCTGACTAGTAGGCCTGCTAGCCTGTTTAAACTGG-TGAGCAAGGGCGAGGAGCTG-3′) and *Pme*I and *Xho*I downstream of Venus (5′-CCGCTCGAGTTACAGTTT-AAACAGGGCGGCGGTCACGAACTCCA-3′). The PCR fragment was subcloned into pTriEx 1.1 – Hygro at *Nco*I and *Xho*I, by screening for a fluorescent colony to form an intermediate vector.
3. Multiple cloning sites were subcloned into the intermediate vector to create pCfvtx by using PCR fragments containing *Spe*I, *Bam*HI, *Stu*I and *Bgl*II, *Sma*I, *Nhe*I sandwiching a stop codon using 5′-end phosphorylated primers (sense: 5′-CTAGTGGATCCAGGCCTTAAAGATCTCCCGGGG-3′ and anti-sense: 5′-CTAGCCCCGGGAGATCTTTAAGGC-

CTGGATCCA-3′). This PCR fragment was subcloned into the intermediate vector at *Spe*I and *Nhe*I. A non-fluorescent colony was selected.

3.2.3. Generating a Cassette Library

Fusion proteins of greater complexity and multiple domains can be easily constructed following a consistent set of protocols (**Fig. 4.3**). Each new cassette becomes part of a growing cassette library.

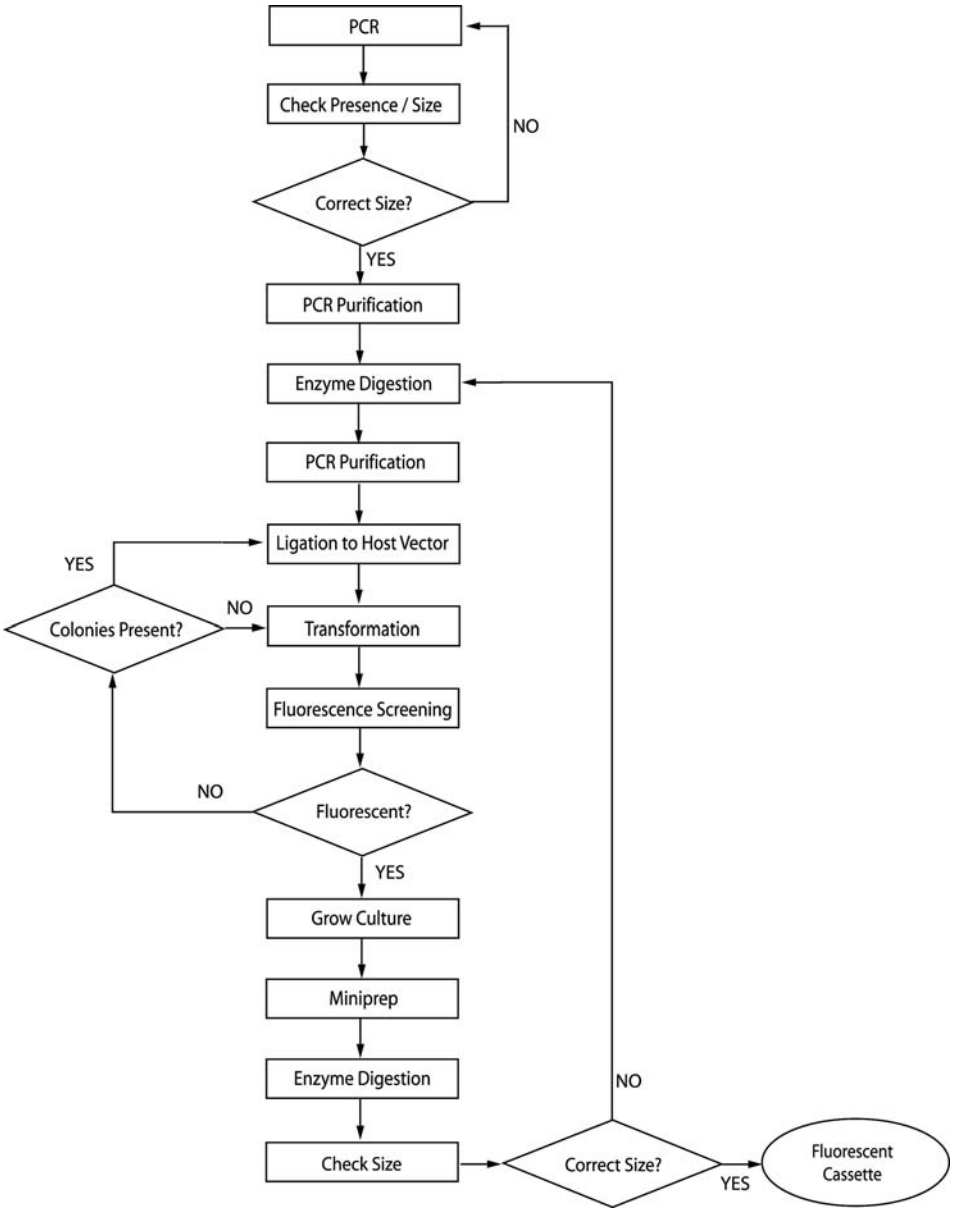

Fig. 4.3. Insertion of a gene into the standard cassette vector. See text for subcloning details.

Insertion of a New Gene of Interest

1. Polymerase chain reaction (PCR): Primers are designed to contain the necessary restriction sites, matching those on pCfvtx, to facilitate insertion into the standard host vector. Annealing temperature, length, and cDNA or plasmid source depend on the gene of interest being amplified. Gene fragments are amplified using the Eppendorf Mastercycler Personal and *Pfu* DNA polymerase. PCR reaction buffer contains 5 μL of 10× PCR buffer with $MgSO_4$ (provided with enzyme), 5 μL each of the 5′–3′ and 3′–5′ primers, 5 μL of 5 mM dNTP, 1 μL of cDNA or plasmid source, 28.5 μL water, and 0.5 μL *Pfu* DNA polymerase.
2. Purification of PCR fragment: The Invitrogen PureLink PCR Purification kit was used to purify PCR fragments. The kit can be used to purify fragments ranging in length from 100 to 12,000 bp. It is highly recommended that a DNA gel (1% agarose gel in 0.5× TAE buffer, 25 min at 100 V) be run to check for the presence of the gene of interest, as well as to assess the specificity of the PCR amplification. The gene of interest should appear as a clear band at the correct size when compared to a DNA ladder. If a blur appears or no band is visible, the PCR conditions should be modified to better amplify the gene.
3. Enzyme digestion: pCfvtx (host vector) and the PCR fragment are digested at corresponding restriction cut sites using restriction enzymes. The reaction buffer consists of 1 μL each of the restriction enzymes, 3 μL of 10× buffer (provided with enzyme), 1 μL 30× BSA buffer (provided with enzyme), and 24 μL water. Digestions are incubated at 37°C for 3 h using the Eppendorf Mastercycler Personal to keep conditions constant.
4. Purification of digested products: The Invitrogen PureLink PCR Purification kit can be used to purify the digested PCR fragment and host vector.
5. Ligation: T4 DNA Ligase is used to ligate the host vector and PCR fragment. The reaction is carried out with 2 μL of ligase buffer (provided with enzyme) and 1 μL T4 DNA ligase at 16°C for 1 h using the Eppendorf Mastercycler Personal to keep conditions constant.
6. Transformation of competent *E. coli* cells: 20 μL aliquots of DH5α *E. coli* cells are stored at –80°C. Prior to transformation, an aliquot is left to slowly thaw on ice (4°C). One microliter of the ligation product is mixed into the competent cell aliquot. Transformation is achieved by heat-shocking the cells, first quickly subjecting the aliquot to

42°C for 40 s and then placing it back on ice for another 5 min.

7. *E. coli* cell culturing: Transformed cells are grown in 1 mL of LB containing 1 μL of 100 μg/mL ampicillin overnight at 37°C in a shaking incubator at 200 rpm.
8. Fluorescence screening: Cell growths are diluted and plated on agar plates. The diluted cell solution is spread onto a pre-warmed plate. The plate is then incubated at 37°C overnight to form colonies. Colonies containing successful subclones are screened by fluorescence using an Illumatool Tunable Lighting System LT-9500. Colonies from a transformation will form both fluorescent and non-fluorescent colonies. Only successful subclones will fluoresce. A fluorescent colony can thus be picked off the plate and grown in 3 μL LB overnight at 37°C.
9. Plasmid purification: The Invitrogen PureLink Quick Plasmid Miniprep kit is used to extract plasmid DNA from *E. coli* cells. Extracted plasmids are stored at –20°C.
10. Size and sequence checking: A purified plasmid from a new insertion subclone can be size-checked by digesting the plasmid at available restriction cut sites on the standard cassette vector for 1.5 h at 37°C. The digested product can be run through a DNA gel and the size of the insertion product verified with a DNA ladder. If the size of the insertion is correct, a final check should be performed by sending the plasmid out for sequencing to ensure there were no frameshifts or other misligations during the subcloning process.

Removing the Fluorescent Protein Gene

1. Enzyme digestion: The fluorescent protein gene can be easily removed (**Fig. 4.4**) by digesting the plasmid at the blunt-end (e.g., *Pme*I) restriction cut site.
2. Purification: The Invitrogen PureLink PCR Purification kit can be used to purify the digested plasmid.
3. Ligation and transformation: The same procedure can be used as in **Section 3.2.3.1** (steps 5–7) to ligate and transform the digested plasmid.
4. Screening: Since the fluorescent protein gene is removed, non-fluorescent colonies should be picked off the plate and grown overnight. The purification of the new, non-fluorescent plasmid remains the same as in **Section 3.2.3.1**. This new plasmid can be added to the growing cassette library.

Recombination of Cassette Plasmids

The availability of compatible cohesive ends allows cassettes to be combined and recombined irrespective of order, each time resulting in a fusion cassette with the same standard restriction

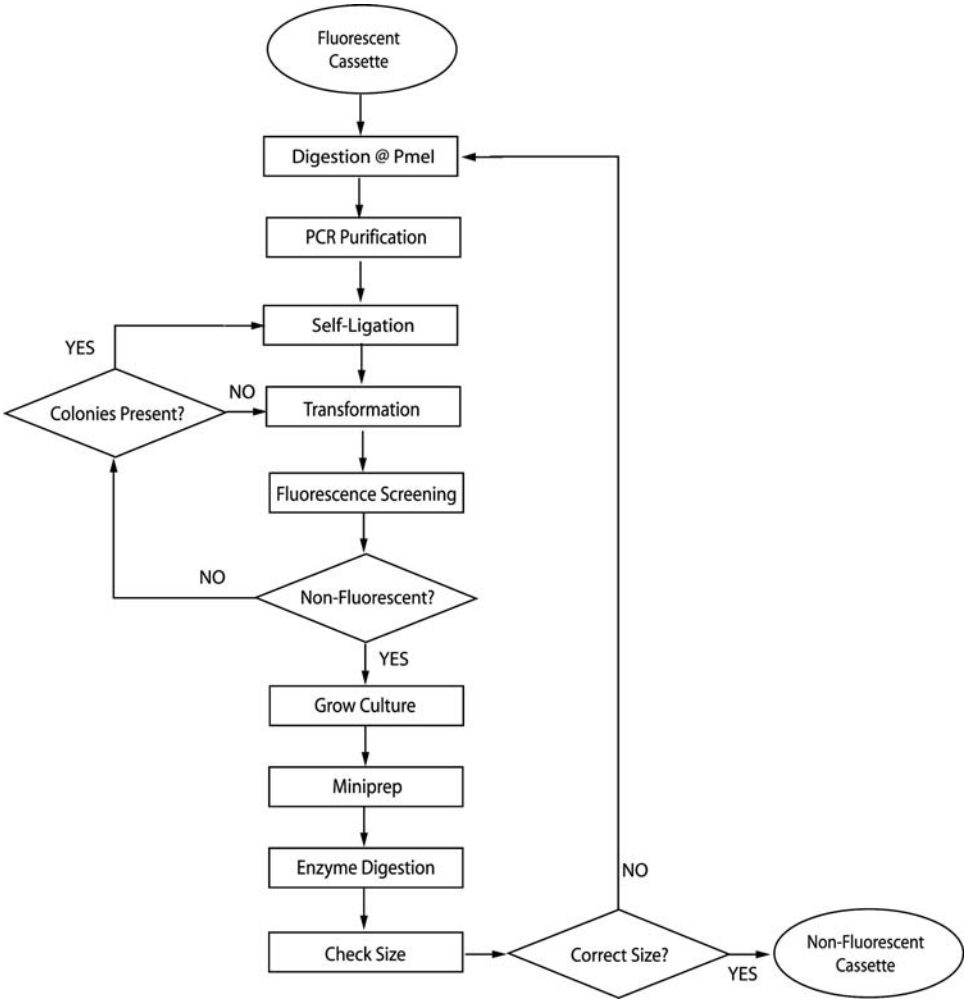

Fig. 4.4. Removal of the fluorescent protein gene. See text for subcloning details.

cut site scheme (**Fig. 4.5a**). There are two ways to create an AB fusion from cassette A and B: ligate the "insert" from cassette B (digested at 2a and 3) to the "host" cassette A (digested at 2b and 3), or ligate the "insert" from cassette A (digested at 1 and 2b) to the "host" cassette B (digested at 1 and 2a) (**Fig. 4.5b**). Creating a BA fusion from cassette A and B follows a similar scheme (**Fig. 4.5c**). Both the resulting AB and BA fusion cassettes will have the same standard vector structure and can be added to the cassette library.

To facilitate easy fluorescence-based screening, the "insert" should be fluorescent, while the "host" should be non-fluorescent (**Fig. 4.6**). Alternatively, both the cassettes can be fluorescent as long as two spectrally different fluorescent genes are used.

1. Digestion of "host" plasmid: The "host" plasmid is digested at restriction cut sites 1 and 2a (the "insert" will be inserted at the 5′-end) or cut sites 2b and 3 (the "insert" will be

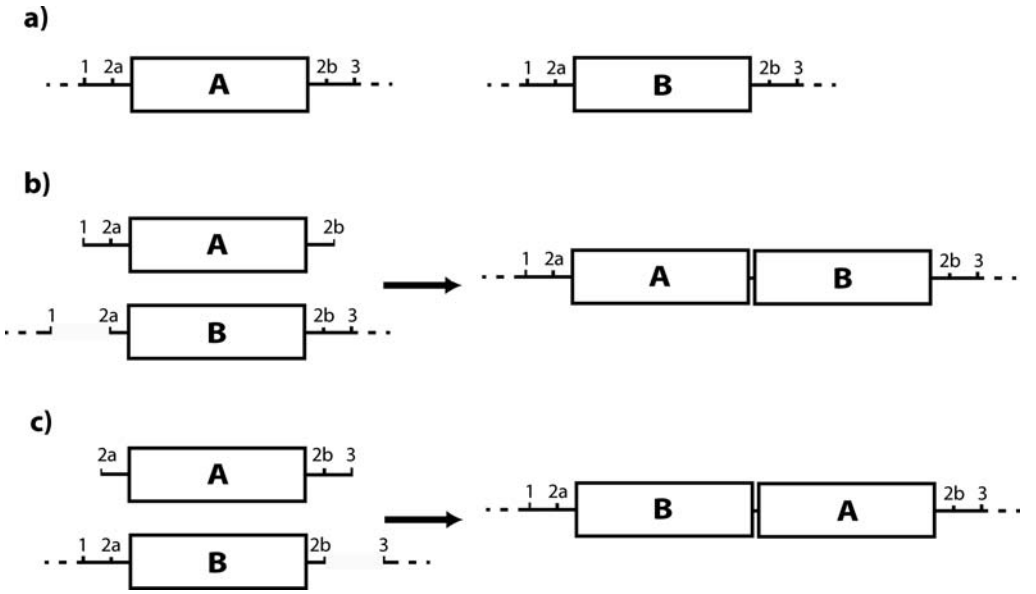

Fig. 4.5. Construction of fusion cassettes. There are two ways to create an AB fusion from available cassettes A and B (**a**). One method is to ligate the insert from cassette A digested at sites 1 and 2b into the host cassette B digested at 1 and 2a (**b**). Ligating the compatible cohesive ends at sites 2a and 2b will result in a sequence unrecognized by either restriction enzyme. A similar method can be used to form a BA fusion (**c**). Any cassette formed from the standard cassette vector will contain the same structure after subcloning.

inserted at the 3′-end). Follow steps 3 and 4 of **Section 3.2.3.1**.

2. Digestion of "insert" plasmid: The insertion fragments should be fluorescent and digested at two restriction cut sites flanking both the gene of interest and the fluorescent protein gene (sites 2a and 3 or 1 and 2b). Step 3 of **Section 3.2.3.1** can be followed to digest the plasmid; however, this digested fragment should be purified differently. The digestion product for this "insert" plasmid will result in both cut insert fragment and the rest of the plasmid with same protruding cohesive ends. To isolate just the insertion fragment, a DNA gel electrophoresis can be run and the insertion fragment excised from the gel. The Invitrogen PureLink Quick Gel Extraction kit can be used to purify the excised gel piece.
3. Ligation and transformation: Follow steps 5–10 of **Section 3.2.3.1**.

3.2.4. Example of Creation of CEcadY12 Ca^{2+} Biosensor

Subcloning CEcadY12 from Cassette Plasmids

1. Following **Section 3.2.3.1**, the following plasmids were previously created and added to the cassette library: pCFPtx (21) contains the gene coding for Cerulean (a variant of CFP) (28); pEcad12vtx (13) contains domains 1 and 2 of epithelial cadherin upstream of Venus.
2. Following **Section 3.2.3.3**, pCFPtx was digested at *Nco*I and *Nhe*I while pEcad12vtx was digested at *Nco*I and

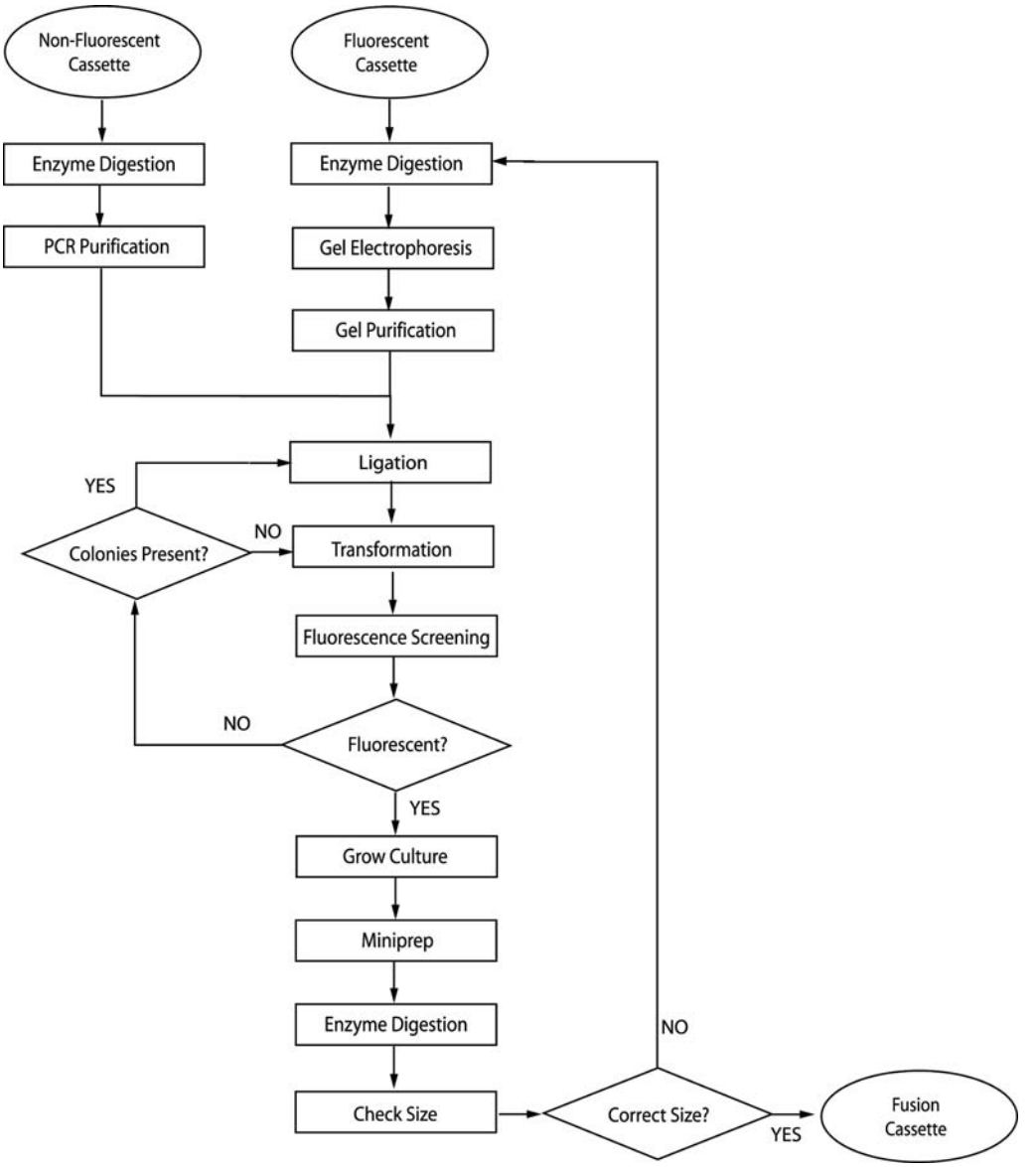

Fig. 4.6. Recombination of existing cassette plasmids into new fusion proteins. See text for subcloning details.

*Spe*I. (Recall: *Spe*I and *Nhe*I produce compatible cohesive ends.)

3. *E. coli* cells were transformed with the ligated plasmid (named pC12Ytx). Colonies with both cyan and yellow fluorescence were screened and selected. pC12Ytx: Cerulean-Ecad12-Venus.

Tagging of Fusion Proteins for Purification (e.g., with Histidine, His, or Glutathione-S-Transferase, GST)

1. The following plasmids were previously created and added to the cassette library: pC12Ytx (13) and pHistx (21), which contains a 6x-His tag.
2. Following **Section 3.2.3.3**, pC12Ytx was digested at *Spe*I and *Xho*I while pHistx was digested at *Nhe*I and *Xho*I.
3. *E. coli* cells were transformed with the ligated plasmid (named pHisC12Ytx). Colonies with both cyan and yellow fluorescence were screened and selected. pHisC12Ytx contains a 6xHis affinity tag that can be used to purify the CEcadY12 biosensor protein using Ni-NTA 6% agarose beads charged with Ni^{2+} ions.

Tagging of Fusion Proteins for Subcellular Localization

1. The following plasmids were previously created and added to the cassette library: pC12Ytx (13) and pTattx (21), which contains a peptide that localizes to the nucleolus and nucleus.
2. Following **Section 3.2.3.3**, pC12Ytx was digested at *Spe*I and *Xho*I while pTattx was digested at *Nhe*I and *Xho*I.
3. *E. coli* cells were transformed with the ligated plasmid (named pTatC12Ytx). Colonies with both cyan and yellow fluorescence were screened and selected. pTatC12Ytx contains a peptide derived from the HIV TAT protein transduction domain that can be used to target the CEcadY12 Ca^{2+} biosensor protein to the nucleolus and nucleus.

3.3. Live-Cell Imaging Using Fluorescence Microscopy

3.3.1. Cell Culture Procedures

These procedures are used for maintaining Cos-7 cells. Dilutions and growth conditions may vary for different cell lines (*see* **Note 8**).

1. Growing cells from stock: Cos-7 cells are stored at –80°C in DMSO. Prior to growing cells in T-25 flasks, thaw cells in a water-bath at 37°C and pre-heat DMEM with 10% FBS growth medium at 37°C. Add 5 mL DMEM with 10% FBS growth medium to T-25 flask. Gently mix thawed cell solution. Slowly add cell solution (10^6–10^7 cells/mL) to T-25 flask dropwise. Gently rock the flask to distribute cells and incubate overnight at 37°C at 5% CO_2. Cells should be about 80–100% confluent by the next day.
2. Passaging cells: Pre-heat DMEM with 10% FBS growth medium, PBS without Ca^{2+}, and trypsin–EDTA at 37°C. Add 5 mL DMEM with 10% FBS growth medium to a new sterile T-25 flask. Remove old growth medium from cell T-25 flask. Gently add 5 mL of PBS to wash cells and remove PBS solution. Add 1 mL of trypsin–EDTA to the flask. Incubate cells for 3 min at 37°C. Rock the flask and tap gently to detach cells from bottom surface. Remove trypsinized cells and place into an eppendorf tube. Centrifuge at 500*g* for

3 min. Remove supernatant, being careful to avoid disturbing the cell pellet. Resuspend cells in 100 μL DMEM with 10% FBS. Add cells at desired dilution ratio to new T-25 flask.

3. Stocking cells: Cells should be at 80–100% confluency. Preheat DMEM with 10% FBS growth medium, PBS without Ca^{2+}, 1 mL of trypsin–EDTA, and 0.5 mL DMSO solution. Remove old growth medium from T-25 flask. Gently add 5 mL of PBS to wash cells and remove PBS solution. Mix 1 mL of trypsin–EDTA solution and add to the flask. Incubate cells for 3 min at 37°C. Rock the flask and tap gently to detach cells from bottom surface. Remove trypsinized cells and place into an eppendorf tube. Centrifuge at 500*g* for 3 min. Remove supernatant, being careful to avoid disturbing the cell pellet. Resuspend cells in 100 μL DMEM with 10% FBS. Remove 50 μL of cell solution and add to a storage tube. Mix DMSO solution and add dropwise to storage tube containing cells. Very gently mix the solution. Freeze storage tube in a styrofoam freezer box at –20°C overnight. The following day, move Styrofoam box to –80°C for long-term storage. Follow step 1 in this section to re-grow cells from stock.

3.3.2. Preparing Cells for Transfection and Imaging

1. Growing cells in glass-bottom wells: When cells are at 80–100% confluency, passage cells as in **Section 3.3.1**. Pre-heat DMEM with 10% FBS growth medium, PBS without Ca^{2+} (Invitrogen), and 1 mL of trypsin–EDTA at 37°C. Add 2 mL DMEM with 10% FBS growth medium to a new sterile glass-bottom well. Remove old growth medium from T-25 flask. Gently add 5 mL of PBS to wash cells and remove PBS solution. Add 1 mL of trypsin–EDTA to flask. Incubate cells for 3 min at 37°C. Rock the flask and tap gently to detach cells from bottom surface. Remove trypsinized cells and place into an eppendorf tube. Centrifuge at 500*g* for 3 min. Remove supernatant, being careful to avoid disturbing the cell pellet.
2. Resuspend cells in 100 μL DMEM with 10% FBS. Add cells at desired dilution ratio to the glass-bottom well. For next day transfection, dilute Cos-7 cells at 1:10.

3.3.3. Transfection

1. Preparing transfection solution: When cells in glass-bottom wells are at 50% confluency, prepare transfection solution using Lipofectin. Mix 2 μg of plasmid with 100 μL of preheated DMEM without FBS. In a separate eppendorf tube, mix 10 μL of Lipofectin solution with 100 μL of DMEM without FBS. Incubate for 30–45 min at room temperature. Mix the two solutions gently and incubate for 15–30 min,

allowing plasmid DNA to complex with the Lipofectin solution.

2. Preparing cells for transfection: Carefully remove old growth medium from glass-bottom wells. Wash cells with 2 mL of DMEM without FBS and remove the solution.
3. Adding transfection solution to washed cells: Gently mix 0.8 mL of DMEM without FBS into incubated transfection solution containing Lipofectin and plasmid DNA. Add this solution gently to the glass-bottom well. Incubate at 37°C with 5% CO_2 for 5–8 h.
4. Growing transfected cells: Remove Lipofectin-containing medium and replace with 2 mL of DMEM with 10% FBS growth medium. Grow transfected cells at 37°C with 5% CO_2 for 12–48 h.

3.3.4. Imaging Experiment

1. Imaging experiment: Set up fluorescence microscope with appropriate filters and objectives (see **Section 2.3**, step 4 for microscope specifications). Prepare software settings for fluorescence measurements as appropriate for the imaging experiment to be performed.
2. Preparing cells for imaging (*see* **Note 9**): Remove old growth medium and wash cells with 1 mL PBS. Add 1.8 mL PBS solution to prevent cells from drying out.
3. Preparing stimulus solution: Dilute stimulus stock solution to 10× desired concentration. For example, if a concentration of 1 μM is required to stimulate cells during imaging, prepare a concentrated solution of 10 μM.
4. During imaging experiment: Add 200 μL stimulant dropwise to glass-bottom well, allowing stimulant solution to diffuse across cells (*see* **Note 10**).
5. Fluorescence measurement: Define regions of interest and monitor fluorescence changes for both donor and acceptor emission channels.

3.3.5. Example of Use of FRET Biosensor to Monitor Ca^{2+} Response

1. Ca^{2+} biosensor construct: A troponin-based Ca^{2+} biosensor named C-TNXL-V was amplified from TN-XL (29) and subcloned into our cassette system. In the presence of Ca^{2+}, C-TNXL-V shows an increase in FRET efficiency; this corresponds to a decrease in CFP emission with a corresponding increase in YFP emission.
2. 10 μM ATP or 1 μM ionomycin can be used to stimulate cells during imaging (**Fig. 4.7a**). A plot of the changes in fluorescence intensity for the CFP and YFP channels is shown in **Fig. 4.7b, c**.

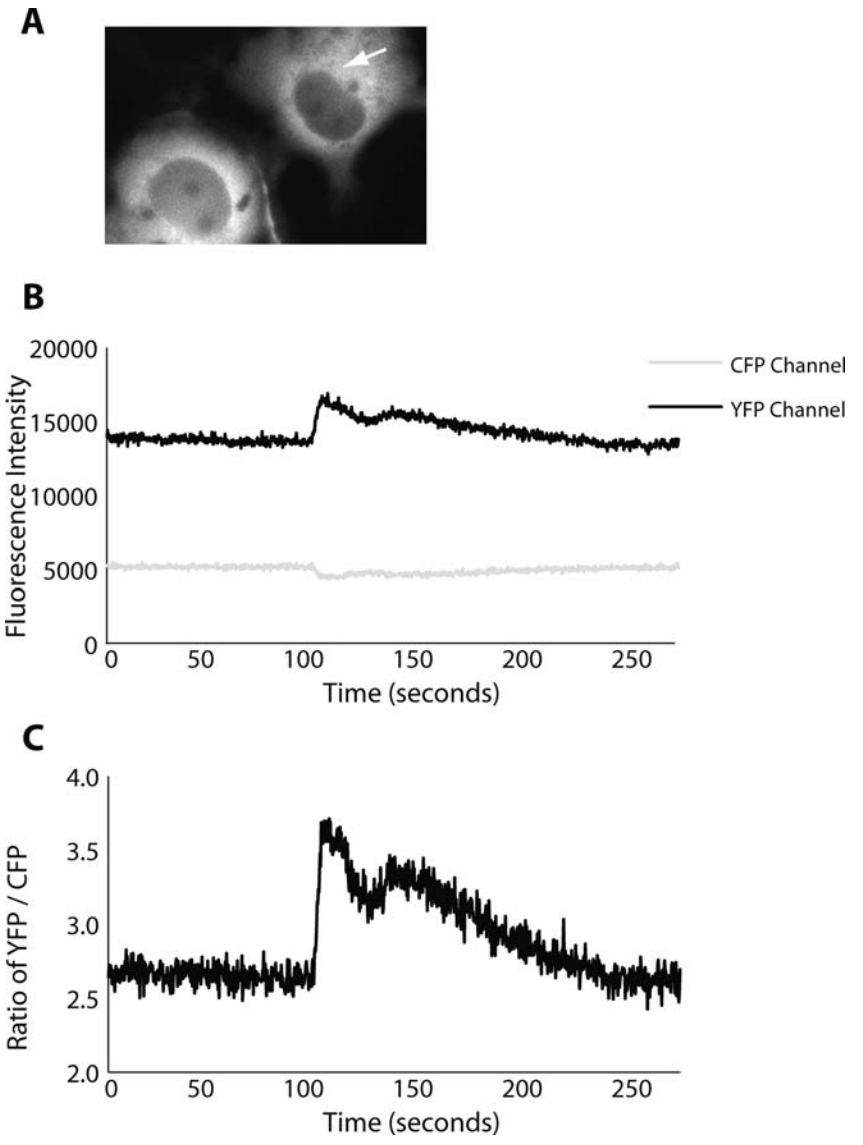

Fig. 4.7. Response of C-TNXL-V biosensor to ATP stimulation. Cos-7 cells were transfected with the C-TNXL-V Ca^{2+} biosensor (**a**). Fluorescence intensities for both the YFP and CFP channels were measured where indicated by an arrow. Ten micromolars of ATP was added to cause a Ca^{2+} response at 100 s (**b**). YFP/CFP ratio changes are also shown (**c**).

3.3.6. Example of Use of FRET Biosensor to Monitor Apoptosis

1. vDEVDc is a caspase-7 FRET biosensor that consists of a CFP and a YFP sandwiching a caspase recognition peptide, Asp-Glu-Val-Asp (DEVD) (16, 18).
2. 5 mM of STS is used to induce apoptosis in Cos-7 cells. During apoptosis, caspase-7, an executioner protease, is activated. In the presence of endogeneous caspase-7, the vDEVDc biosensor is cleaved, separating the fluorescent pair and causing a decrease in FRET efficiency. **Figure 4.8b, c** shows

an increase in CFP emission with a corresponding decrease in YFP emission upon cleavage.

3. Corresponding morphological changes can also be observed, confirming apoptotic changes within the cell (16, 22) (**Fig. 4.8a**).

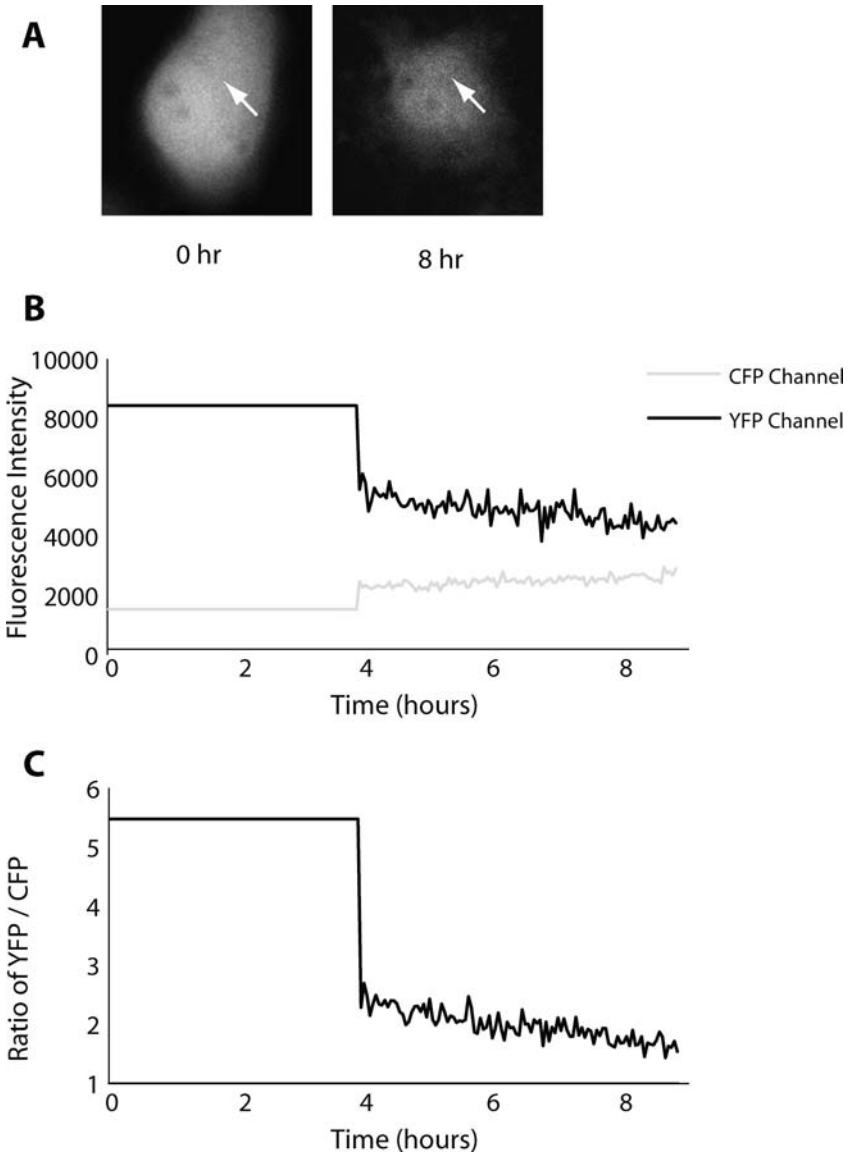

Fig. 4.8. Response of vDEVDc biosensor to STS-induced apoptosis. Cos-7 cells were transfected with the vDEVDc caspase biosensor. Cell images are taken before (*left*) and after (*right*) STS-induced apoptosis (**a**). Fluorescence intensities for both the YFP and CFP channels were measured where indicated by an *arrow* (**b**). YFP/CFP ratio changes are also shown (**c**).

4. Notes

1. Store all enzymes at –20°C. To prevent cross-contamination, we often aliquot the solutions into smaller eppendorf tubes that are clearly labeled. This prevents the contamination of larger volumes.
2. Unless otherwise stated, store growth medium (DMEM with or without FBS) at 4°C and all other cell culture solutions at –20°C. To prevent repeated cycles of thawing and freezing, aliquot these solutions into smaller tubes, for instance, trypsin–EDTA is aliquoted into 1 mL aliquots since this is the amount needed for each passage.
3. Make sure to immediately clean off unused oil from objectives using lens paper sprayed with ethanol. The buildup of oil is much harder to clean off and will affect cell images taken.
4. The number of models generated for each biosensor was deemed sufficient when doubling the number of generated models did not change the overall average obtained (13).
5. Developing a computational tool that outputs the distance and orientation factors in addition to the FRET efficiency allows other biosensor characteristics to be studied. For instance, the conformational change of CEcadY12 involves homodimerization in the presence of Ca^{2+}. Closer inspection of the Ca^{2+}-bound models revealed a shorter, more restrained distance between the CFP and the YFP (91 Å versus 85 Å). This restrained distance is caused by limited rotational freedom of the linkers in the presence of Ca^{2+} as observed from the change in orientation factor from 0.59 to 0.39 (13).
6. We often use Venus instead of other YFP variants because it matures (folds) faster and is a generally brighter variant.
7. Another standard vector that was created is pCfcerutx3, which has the same structure as pCfvtx with the Venus gene replaced by a gene coding for Cerulean, a variant to CFP (28). Instead of the base vector pTriEx 1.1 – Hygro, pTriEx 3 – Hygro (Novagen) was used.
8. Perform all cell-culture steps in a laminar hood to prevent contamination.
9. Leave cells in growth medium until ready to image. Removal of growth medium too early will cause cells to detach from the glass surface. Similarly, it is important to add and remove solutions very slowly and gently to prevent detaching cells.

10. When adding stimulants, be careful not to disturb the surface of the PBS solution, as this will cause a noticeable change in measured fluorescence intensity levels. Similarly, be careful not to touch any part of the microscope setup, as measurements are also sensitive to small vibrations.

Acknowledgments

This work was supported by a fellowship to EP from National Science and Engineering Research Council (NSERC) and grants to KT from the Canadian Foundation of Innovation (#10296), Canadian Institutes of Health Research (#81262), Heart and Stroke Foundation (#NA6241), and the National Science and Engineering Research Council (#283170).

References

1. Griesbeck, O. (2004) Fluorescent proteins as sensors for cellular functions. *Curr Opin Neurobiol.* **14**, 636–41.
2. Li, I. T., Pham, E., and Truong, K. (2006) Protein biosensors based on the principle of fluorescence resonance energy transfer for monitoring cellular dynamics. *Biotechnol Lett.* **28**, 1971–82.
3. Luo, K. Q., Yu, V. C., Pu, Y., and Chang, D. C. (2001) Application of the fluorescence resonance energy transfer method for studying the dynamics of caspase-3 activation during UV-induced apoptosis in living HeLa cells. *Biochem Biophys Res Commun.* **283**, 1054–60.
4. Miyawaki, A. (2003) Visualization of the spatial and temporal dynamics of intracellular signaling. *Dev Cell.* **4**, 295–305.
5. Pozzan, T., Mongillo, M., and Rudolf, R. (2003) The Theodore Bucher lecture. Investigating signal transduction with genetically encoded fluorescent probes. *Eur J Biochem.* **270**, 2343–52.
6. Truong, K., and Ikura, M. (2001) The use of FRET imaging microscopy to detect protein-protein interactions and protein conformational changes in vivo. *Curr Opin Struct Biol.* **11**, 573–8.
7. Kurokawa, K., Mochizuki, N., Ohba, Y., Mizuno, H., Miyawaki, A., and Matsuda, M. (2001) A pair of fluorescent resonance energy transfer-based probes for tyrosine phosphorylation of the CrkII adaptor protein in vivo. *J Biol Chem.* **276**, 31305–10.
8. Clegg, R. M. (1995) Fluorescence resonance energy transfer. *Curr Opin Biotechnol.* **6**, 103–10.
9. Tsien, R. Y. (1998) The green fluorescent protein. *Annu Rev Biochem* **67**, 509–44.
10. Berridge, M. J., Lipp, P., and Bootman, M. D. (2000) The versatility and universality of calcium signalling. *Nat Rev Mol Cell Biol.* **1**, 11–21.
11. Miyawaki, A., Griesbeck, O., Heim, R., and Tsien, R. Y. (1999) Dynamic and quantitative Ca^{2+} measurements using improved cameleons. *Proc Natl Acad Sci USA* **96**, 2135–40.
12. Miyawaki, A., Llopis, J., Heim, R., McCaffery, J. M., Adams, J. A., Ikura, M., and Tsien, R. Y. (1997) Fluorescent indicators for Ca^{2+} based on green fluorescent proteins and calmodulin. *Nature* **388**, 882–7.
13. Pham, E., Chiang, J., Li, I., Shum, W., and Truong, K. (2007) A computational tool for designing FRET protein biosensors by rigid-body sampling of their conformational space. *Structure* **15**, 515–23.
14. Kuboniwa, H., Tjandra, N., Grzesiek, S., Ren, H., Klee, C. B., and Bax, A. (1995) Solution structure of Ca^{2+}-free calmodulin. *Nat Struct Biol.* **2**, 768–76.
15. Wriggers, W., Mehler, E., Pitici, F., Weinstein, H., and Schulten, K. (1998) Structure and dynamics of calmodulin in solution. *Biophys J.* **74**, 1622–39.
16. Li, I. T., Pham, E., Chiang, J. J., and Truong, K. (2008) FRET evidence that an isoform of caspase-7 binds but does not cleave its sub-

strate. *Biochem Biophys Res Commun.* **373**, 325–9.
17. Truong, K., Sawano, A., Mizuno, H., Hama, H., Tong, K. I., Mal, T. K., Miyawaki, A., and Ikura, M. (2001) FRET-based in vivo Ca^{2+} imaging by a new calmodulin-GFP fusion molecule. *Nat Struct Biol.* **8**, 1069–73.
18. Chiang, J. J., and Truong, K. (2006) Computational modeling of a new fluorescent biosensor for caspase proteolytic activity improves dynamic range. *IEEE Trans Nanobiosci* **5**, 41–5.
19. Xu, X., Gerard, A. L., Huang, B. C., Anderson, D. C., Payan, D. G., and Luo, Y. (1998) Detection of programmed cell death using fluorescence energy transfer. *Nucleic Acids Res.* **26**, 2034–5.
20. Winters, D. L., Autry, J. M., Svensson, B., and Thomas, D. D. (2008) Interdomain fluorescence resonance energy transfer in SERCA probed by cyan-fluorescent protein fused to the actuator domain. *Biochemistry* **47**, 4246–56.
21. Truong, K., Khorchid, A., and Ikura, M. (2003) A fluorescent cassette-based strategy for engineering multiple domain fusion proteins *BMC Biotechnol.* **3**, 8.
22. Chiang, J. J., and Truong, K. (2005) Using co-cultures expressing fluorescence resonance energy transfer based protein biosensors to simultaneously image caspase-3 and Ca^{2+} signaling. *Biotechnol Lett.* **27**, 1219–27.
23. Violin, J. D., Zhang, J., Tsien, R. Y., and Newton, A. C. (2003) A genetically encoded fluorescent reporter reveals oscillatory phosphorylation by protein kinase C *J Cell Biol.* **161**, 899–909.
24. Presley, J. F., Cole, N. B., Schroer, T. A., Hirschberg, K., Zaal, K. J., and Lippincott-Schwartz, J. (1997) ER-to-Golgi transport visualized in living cells. *Nature* **389**, 81–5.
25. Dale, R. E., Eisinger, J., and Blumberg, W. E. (1979) The orientational freedom of molecular probes. The orientation factor in intramolecular energy transfer. *Biophys J.* **26**, 161–93.
26. Hillel, Z., and Wu, C. W. (1976) Statistical interpretation of fluorescence energy transfer measurements in macromolecular systems. *Biochemistry* **15**, 2105–13.
27. Nagai, T., Ibata, K., Park, E. S., Kubota, M., Mikoshiba, K., and Miyawaki, A. (2002) A variant of yellow fluorescent protein with fast and efficient maturation for cell-biological applications. *Nat Biotechnol.* **20**, 87–90.
28. Rizzo, M. A., Springer, G. H., Granada, B., and Piston, D. W. (2004) An improved cyan fluorescent protein variant useful for FRET. *Nat Biotechnol.* **22**, 445–9.
29. Mank, M., Reiff, D. F., Heim, N., Friedrich, M. W., Borst, A., and Griesbeck, O. (2006) A FRET-based Ca^{2+} biosensor with fast signal kinetics and high fluorescence change. *Biophys J.* **90**, 1790–6.